



A new fluorescence “turn-on” type chemosensor for Fe³⁺ based on naphthalimide and coumarin



Zhengqian Li, Ying Zhou, Kai Yin, Zhu Yu, Yan Li, Jun Ren*

Hubei Collaborative Innovation Center for Advanced Organic Chemical Materials – College of Chemistry and Chemical Engineering, Hubei University, Wuhan 430062, PR China

ARTICLE INFO

Article history:

Received 8 October 2013
Received in revised form
25 December 2013
Accepted 29 December 2013
Available online 8 January 2014

Keywords:

Fluorescent sensor
Turn-on
Chemosensor
Ferric ion
Naphthalimide
Coumarin

ABSTRACT

A new Fe³⁺-selective “turn-on” chemosensor **1** based on coumarin and naphthalimide was designed and synthesized. The chemosensor exhibits high selectivity for Fe³⁺ over other ions (Mn²⁺, Co²⁺, Ni²⁺, Cu²⁺, Ag⁺, Cd²⁺, Pb²⁺, Ca²⁺, Al³⁺, Ba²⁺, Hg²⁺, Li⁺, Mg²⁺, Sr²⁺, Zn²⁺ and K⁺) with fluorescence-enhancement in THF-H₂O solution. The binding ratio of **1**-Fe³⁺ complex was determined to be 1:1 according to the Job plot. The association constant *K*_a of Fe³⁺ binding with sensor **1** was (2.589 ± 0.206) × 10³ M⁻¹. The detection limit was calculated to be 0.388 μM.

© 2014 Elsevier Ltd. All rights reserved.

1. Introduction

As one of the most essential trace elements in biological systems, ferric ion performs a major role in the growth and development of living systems as well as in many biochemical processes at the cellular level [1,2]. An overload of Fe³⁺ leads to some dysfunction of certain organs, such as heart, pancreas, and liver [3–5]. While, the deficiency of Fe³⁺ causes anemia, hemochromatosis, liver damage, diabetes, and Parkinson's disease [6]. The traditional techniques for determination of Fe³⁺, such as FAAS [7], CE [8], and ICP-AES [9], are complicated and not suitable for quick and online monitoring. Therefore, great importance is attached to developing analytical methods for the convenient and rapid analysis of Fe³⁺.

Fluorescent detection has become the promising strategy used for Fe³⁺ detection [4,5] due to its easy monitoring, low cost and high selectivity. In recent years, considerable efforts have been devoted to the development of fluorescent chemosensors for ferric [10–14]. Generally, it is believed that chemosensors with fluorescence enhancement are much more effective when combining or reacting with the analytes. However, the examples of Fe³⁺-selective “turn-on” chemosensors are still scarce because of the fluorescence quenching of the paramagnetic nature of Fe³⁺ [15–18].

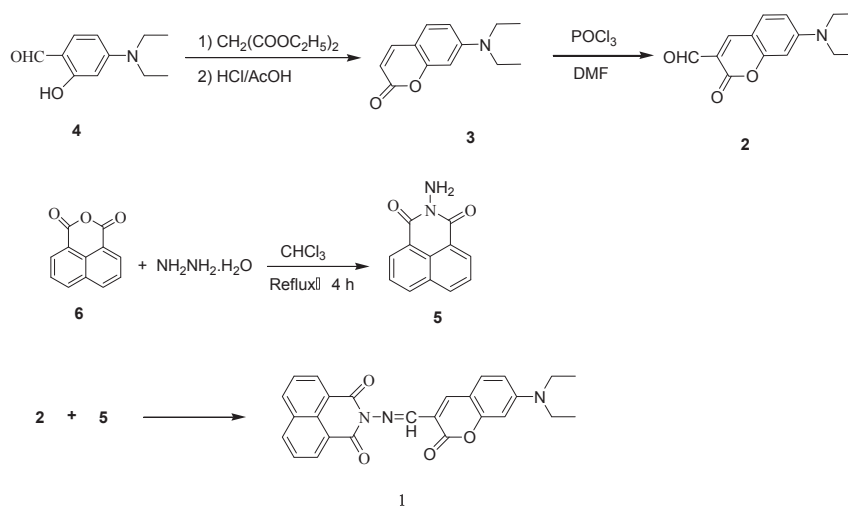
Herein, in this paper we report a new fluorescence “turn-on” type sensor **1** for Fe³⁺ based on Schiff base as bridge, which was synthesized by the condensation of 7-diethylaminocoumarin-3-aldehyde **2** and *N*-aminonaphthalimide **5** in high yield (Scheme 1). Coumarin and naphthalimide are commercial material and they exhibit outstanding chemical, thermal and photochemical stabilities as well as their fluorescence quantum yield [19–23]. On the other hand, oxygen heteroatoms of C=O group on coumarin and naphthalimide could act as chelating sites. Schiff base group was introduced because C=N bond was easily isomerized in the excited state and exhibited weak fluorescence. But when they combined with metal ions and formed metal complexes, the C=N isomerization was inhibited which led to fluorescence changes. The sensor **1** exhibits high selectivity for Fe³⁺ over other ions with fluorescence-enhancement in THF-H₂O solution.

2. Materials and methods

2.1. Experimental

All reagents were purchased from commercial suppliers and were used without further purification except POCl₃ and DMF which were purified according to standard procedures and freshly distilled prior to use. Double distilled water was used throughout the experiment. The solutions of metal ions were prepared from

* Corresponding author. Tel.: +86 27 88662747; fax: +86 27 88663043.
E-mail addresses: renjun@hubu.edu.cn, rj77ll@hotmail.com (J. Ren).



Scheme 1. The synthetic route of compound **1**.

their chloride salts and nitrate salts. Fluorescence detections were performed on Perkin-Elmer LS 50B fluorescence spectrophotometer. Absorbance detections were carried out on a Shimadzu UV-1700 spectrophotometer. The ^1H NMR spectroscopy study was conducted with a Varian INOVA-400 spectrometer using tetramethylsilane (TMS; $\delta = 0$ ppm) as internal standard. All measurements were carried out at room temperature (~ 298 K).

2.2. Synthesis

2.2.1. Synthesis of *N*-aminonaphthalimide (**5**) [24]

5.0 g (25.2 mmol) of 1,8-naphthalic anhydride was dissolved in 160 mL chloroform and stirred at room temperature for 15 min. Then, 3.16 g of hydrazine hydrate (51 mmol) was added to the above solution. The reaction mixture was refluxed in a water bath for 4 h monitoring with thin layer chromatography (TLC). After cooling to room temperature, yellow solid was collected by filtration, washed with chloroform (10 mL \times 3) and dried in vacuum (4.79 g, 89.5% yield). ^1H NMR (400 MHz, DMSO- d_6): δ (ppm) 8.49 (d, 2H, $J = 8.0$ Hz), 8.45 (d, 2H, $J = 8.0$ Hz), 7.86 (t, 2H, $J = 8.0$ Hz), 5.79 (s, 2H, $-\text{NH}_2$).

2.2.2. Synthesis of 7-diethylaminocoumarin (**3**) [25]

To the solution of diethylmalonate (6.4 g, 40 mmol) in EtOH (60 mL), 4-diethylaminosalicylaldehyde (3.86 g, 20 mmol) and piperidine (2 mL) were added and refluxed for 6 h. After the solvent was removed, glacial acetic acid (40 mL) and concentrated HCl (40 mL) were added and stirred for another 6 h. The solution was cooled to room temperature and poured into 200 mL ice-water. 40% NaOH solution was added dropwisely to adjust pH of the solution to about 5, and gray precipitate formed immediately. After stirring for 30 min, the mixture was filtered, washed with water and recrystallized from toluene to give **3** (3.26 g, 75.2% yield). ^1H NMR (400 MHz, CDCl_3) δ (ppm) 7.55 (d, $J = 10.8$ Hz, 1H, $-\text{CH}=\text{C}$), 7.23 (d, $J = 8.8$ Hz, 1H), 6.59 (dd, $J = 8.8$ Hz, 2.4 Hz, 1H), 6.51 (d, $J = 2.4$ Hz, 1H), 6.06 (d, $J = 10.8$ Hz, 1H, $=\text{CH}$), 3.42 (q, $J = 7.2$ Hz, 4H, $-\text{CH}_2\text{CH}_3$), 1.21 (t, $J = 7.2$ Hz, 6H, $-\text{CH}_2\text{CH}_3$).

2.2.3. Synthesis of 7-diethylaminocoumarin-3-aldehyde (**2**) [25]

Anhydrous DMF (2.4 mL) was added dropwise to POCl_3 (2.4 mL) at 30°C under N_2 and stirred for 30 min. To the above solution, compound **3** (1.8 g, 8.29 mmol) in DMF (12 mL) was added. The mixture was stirred at 60°C for 12 h and then poured into 120 mL

ice-water. NaOH solution (20%) was added to adjust the pH of the mixture to yield large amount of precipitate. The crude product was filtered, washed with water and recrystallized from absolute ethanol to give **2** (1.46 g, 5.95 mmol) in 71.8% yield. ^1H NMR (400 MHz, CDCl_3): δ (ppm) 10.13 (s, 1H, $-\text{CHO}$), 8.27 (s, 1H, $-\text{CH}=\text{C}$), 7.42 (d, $J = 9.0$ Hz, 1H), 6.65 (dd, $J = 9.0$ Hz, 2.4 Hz, 1H), 6.49 (d, $J = 2.4$ Hz, 1H), 3.48 (q, $J = 7.2$ Hz, 4H, $-\text{CH}_2\text{CH}_3$), 1.26 (t, $J = 7.2$ Hz, 6H, $-\text{CH}_2\text{CH}_3$).

2.2.4. Synthesis of compound **1**

Compound **2** (1.16 g, 4.73 mmol) was dissolved in 50 mL of hot ethanol, then compound **5** (1.0 g, 4.71 mmol) was added to the solution. The mixture was stirred at room temperature for 30 min, and the gray solid was precipitated. After filtration, the solid was collected, washed successively with ethanol and dried in vacuum to give compound **1** in 91.5% yield (1.89 g). ^1H NMR (400 MHz, CDCl_3): δ (ppm) 8.76 (s, $-\text{N}=\text{CH}$, 1H), 8.74 (s, 1H), 8.67 (d, $J = 7.2$ Hz, 2H), 8.26 (d, $J = 7.2$ Hz, 2H), 7.79 (t, $J = 7.2$ Hz, 2H), 7.42 (d, $J = 8.8$ Hz, 1H), 6.63 (dd, $J = 8.8$ Hz, 2.4 Hz, 1H), 6.50 (s, 1H), 3.48 (q, $J = 8.0$ Hz, 4H), 1.26 (t, $J = 8.0$ Hz, 6H). ^{13}C NMR (100 MHz, CDCl_3): δ (ppm) 188.1, 166.4, 161.4, 158.3, 152.6, 145.5, 143.0, 134.5, 132.6, 132.0, 131.7, 131.5, 127.2, 122.8, 111.4, 110.3, 110.0, 108.7, 97.3, 45.3, 12.6. MS (ESI): $m/z = 440.4$ [$\text{M} + 1$] $^+$. Anal. Calcd. for $\text{C}_{26}\text{H}_{21}\text{N}_3\text{O}_4$: C 71.06, H 4.82, N 9.56; Found C 71.12, H 5.01, N 9.45.

2.3. Preparation of solutions for absorption and fluorescence detections

All measurements of spectra were carried out in mixed aqueous solution of THF- H_2O (1/1, v/v). 0.1 mmol of each inorganic salt ($\text{Al}(\text{NO}_3)_3$, ZnCl_2 , HgCl_2 , AgNO_3 , KCl , $\text{NiCl}_2 \cdot 6\text{H}_2\text{O}$, PbCl_2 , $\text{CaCl}_2 \cdot 2\text{H}_2\text{O}$, $\text{BaCl}_2 \cdot 2\text{H}_2\text{O}$, $\text{MgCl}_2 \cdot 6\text{H}_2\text{O}$, CdCl_2 , $\text{CoCl}_2 \cdot 6\text{H}_2\text{O}$, $\text{LiCl} \cdot \text{H}_2\text{O}$, $\text{CuCl}_2 \cdot 2\text{H}_2\text{O}$, $\text{MnCl}_2 \cdot 4\text{H}_2\text{O}$, $\text{SrCl}_2 \cdot 6\text{H}_2\text{O}$ and FeCl_3) was dissolved in distilled water (8 mL) to afford 1.25×10^{-2} mol/L aqueous solution. Further dilutions were made to prepare 5.96×10^{-4} mol/L solutions for the experiments. The stock solution of compound **1** was prepared by dissolving 26.2 mg compound **1** in 100 mL dry THF and subsequently, 10.0 mL of the solution was then transferred to a 100 mL volumetric flask, diluted to the mark with dry THF. Absorption and fluorescence detections were made using a 5.0 mL cuvette. For all measurements of fluorescence spectra, excitation wavelength was 456 nm. The excitation and emission wavelength bandpasses were both set at 5.0 nm.

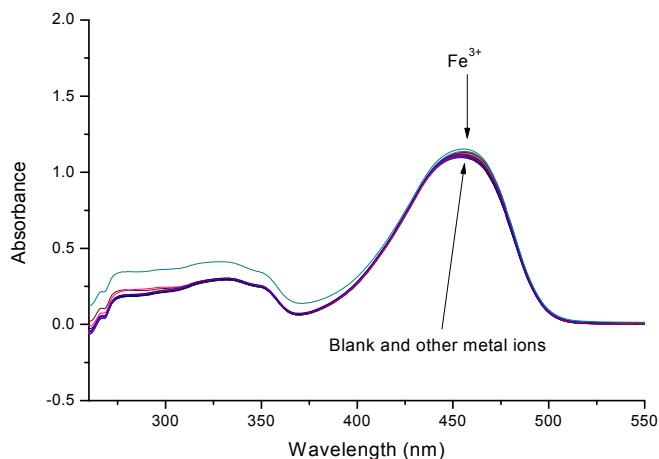


Fig. 1. UV–Vis absorption of **1** (5.96×10^{-5} M) in the presence of different metal ions (10 equiv. each) in THF–H₂O solution (1:1, v/v).

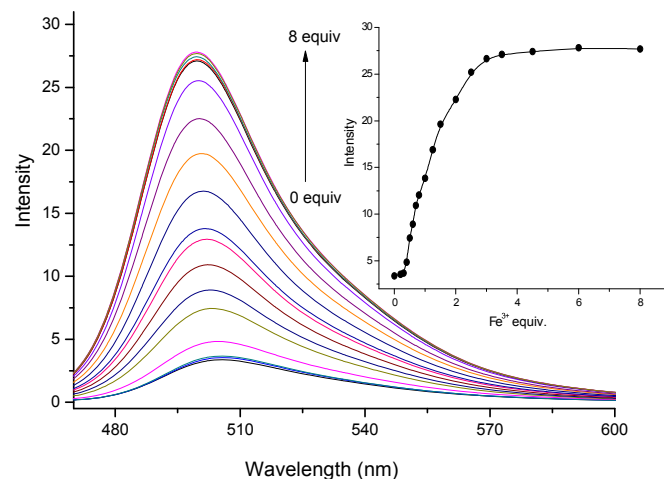


Fig. 3. Fluorescent spectra of **1** (5.96×10^{-5} M) with the addition of various concentration of Fe³⁺ in THF–H₂O (1:1, v/v) ($\lambda_{\text{ex}} = 456$ nm). Inset: Changes in the emission intensity at 504 nm.

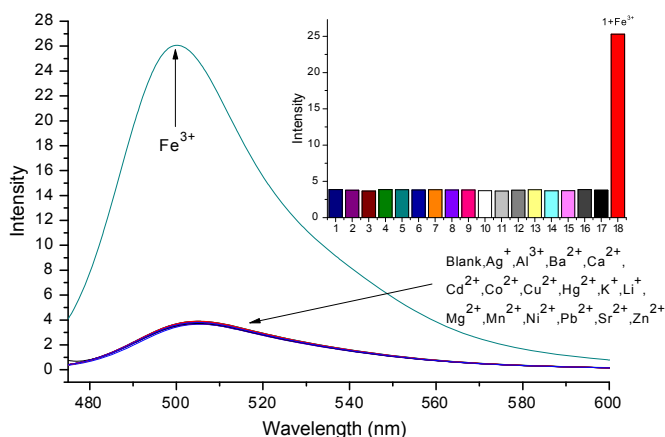


Fig. 2. Fluorescence spectra of **1** (5.96×10^{-5} M) in the presence of 10 eq. different metal ions in THF–H₂O solution (1:1, v/v), $\lambda_{\text{ex}} = 456$ nm.

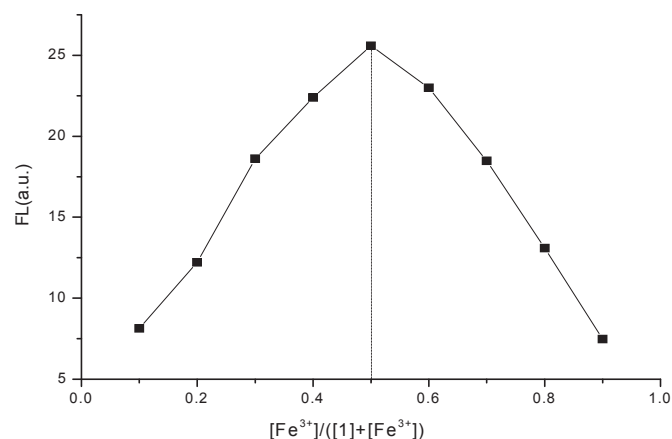


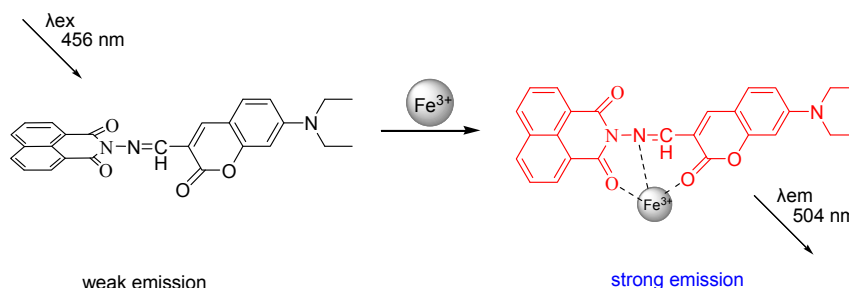
Fig. 4. Job plot for determining the stoichiometry of **1** and Fe³⁺ ion in THF–H₂O solution (1:1, v/v), $\lambda_{\text{ex}} = 456$ nm.

3. Results and discussion

3.1. Spectral studies

The binding behavior of compound **1** was studied towards different metal ions (Fe³⁺, Mn²⁺, Co²⁺, Ni²⁺, Cu²⁺, Ag⁺, Cd²⁺, Pb²⁺, Ca²⁺, Al³⁺, Ba²⁺, Hg²⁺, Li⁺, Mg²⁺, Sr²⁺, Zn²⁺ and K⁺) as their chloride or nitrate salts by absorption and fluorescence spectroscopy. There was no obvious change in UV–Vis absorption spectra of sensors **1** in the presence of any cation as shown in Fig. 1.

The fluorescence spectrum of compound **1** exhibited weak fluorescence emission when excited at 456 nm in THF–H₂O solution (1:1, v/v) (Fig. 2). Upon addition of Fe³⁺ ions to the solution of compound **1**, remarkable enhancement of emission intensity was observed at 504 nm. Under the same conditions as used for Fe³⁺, no significant change of the fluorescence spectrum was observed in the presence of other metal ions, indicating a Fe³⁺-selective OFF–ON fluorescent signaling behavior. The increase of emission intensity may be attributed to the formation of the compound **1**–Fe³⁺



Scheme 2. Possible binding mode of sensor **1** with Fe³⁺.

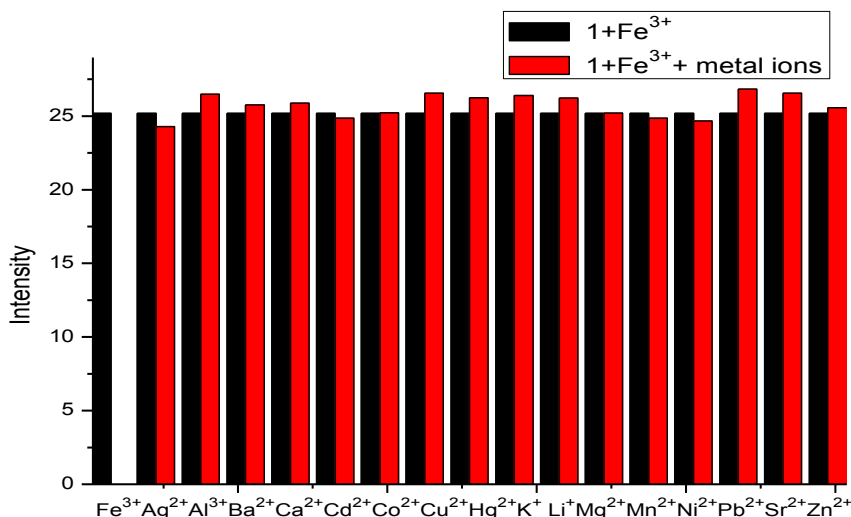


Fig. 5. Fluorescence response of **1** (1.49×10^{-5} M) to various cations in THF-H₂O solution (1:1, v/v), $\lambda_{\text{ex}} = 456$ nm. The black bars represent the fluorescent intensity of **1** and Fe³⁺ (1:1, v/v, 1.49×10^{-5} M). The red bars represent the fluorescence changes that occur upon the addition of competing ions to the solution containing **1** and Fe³⁺ (1:1, 1.49×10^{-5} M). (For interpretation of the references to color in this figure legend, the reader is referred to the web version of this article.)

complex via the oxygen atom on C=O group and nitrogen atom on C=N group as shown in Scheme 2. The coordination of Fe³⁺ and **1** can enhance the coplanarity of naphthalimide and coumarin, which could reduce the nonradiative decay of the excited state and lead to the pronounced fluorescence enhancement [26,27]. To obtain more insight into the fluorescent properties, the fluorescence titration curve of **1** toward Fe³⁺ was investigated (Fig. 3). With increasing concentrations of Fe³⁺, the fluorescence intensity of sensor **1** at λ_{max} 504 nm was gradually increased. Fig. 3 (inset) showed that there was a good linearity between the fluorescence intensity at 504 nm and concentrations of Fe³⁺ in the range from 12 μM to 149 μM , indicating that sensor **1** could detect Fe³⁺ ion quantitatively.

In order to determine the stoichiometry of **1**-Fe³⁺ complex, the method of continuous variation (Job plot) was introduced. The fluorescence intensity at 504 nm was plotted against the molar fraction of sensor **1**, and the total concentration of the sensor and Fe³⁺ ion maintained a constant at 5.96×10^{-5} M. The maximum emission intensity was reached at a molar fraction of 0.5 (Fig. 4), indicating that sensor **1** formed a 1:1 complex with Fe³⁺.

Detection limit (DL) and association constant (K_a) can be also obtained from the fluorescence titration. The detection limit (DL) of sensor **1** for Fe³⁺ was calculated as 0.388 μM by the Stern–Volmer plot [28]:

$$\text{DL} = 3\sigma/S = 3.88 \times 10^{-7} \text{M}$$

where σ is the standard deviation of the blank solution, S is the slope of the calibration curve.

The association constant (K_a) of **1**-Fe³⁺ complex was calculated by the Benesi–Hildebrand Eq. (1) [27]:

$$\frac{1}{F - F_0} = \frac{1}{K_a \times (F_{\text{max}} - F_0) \times [\text{Fe}^{3+}]^n} + \frac{1}{F_{\text{max}} - F_0} \quad (1)$$

where F is the fluorescence intensity at 504 nm at any given Fe³⁺ concentration, F_0 is the fluorescence intensity at 504 nm in the absence of Fe³⁺, and F_{max} is the maximum fluorescence intensity at 504 nm in the presence of Fe³⁺ in solution. The association constant K_a was evaluated graphically by plotting $1/(F - F_0)$ against $1/[\text{Fe}^{3+}]$.

Data were linearly fitted according to Eq. (1) and the K_a value was $(2.589 \pm 0.206) \times 10^3 \text{M}^{-1}$.

3.2. The interference from other metal ions

For an excellent chemosensor, high selectivity is a matter of necessity. To confirm the selectivity of sensor **1**, the competition experiments were also measured by addition of one equivalent of other metal ions, such as Mn²⁺, Co²⁺, Ni²⁺, Cu²⁺, Ag⁺, Cd²⁺, Pb²⁺, Ca²⁺, Al³⁺, Ba²⁺, Hg²⁺, Li⁺, Mg²⁺, Sr²⁺, Zn²⁺ and K⁺, to the THF-H₂O solution of **1** in the presence of one equivalent of Fe³⁺. As shown in Fig. 5, we found that all the coexistent metal ions had no obvious interference with the detection of Fe³⁺. These results indicated that sensor **1** displayed an excellent selectivity toward Fe³⁺.

4. Conclusion

In summary, we have successfully designed a new chemosensor based on coumarin and naphthalimide allowing the specific detection of Fe³⁺ ion. This sensor displayed an excellent selectivity for Fe³⁺ over other metal ions. With increasing concentrations of Fe³⁺, the fluorescence intensity at λ_{max} 504 nm was gradually enhanced. The binding ratio of **1**-Fe³⁺ complex was determined to be 1:1 according to the Job plot. This makes the simple and quick detection of Fe³⁺ ion possible.

Acknowledgments

This work was supported by Natural Science Foundation of Hubei Province of China (No. 2013CFB005).

References

- [1] D'Autréaux B, Tucker NP, Dixon R, Spiro SA. Non-haem iron centre in the transcription factor NorR senses nitric oxide. *Nature* 2005;437:769–72.
- [2] Lee JW, Helmann JD. The PerR transcription factor senses H₂O₂ by metal catalysed histidine oxidation. *Nature* 2006;440:363–7.
- [3] Halliwell B. Reactive oxygen species and central nervous system. *J Neurochem* 1992;59:1609–23.
- [4] Weinberg ED. The role of iron in cancer. *Eur J Cancer Prev* 1996;5:19–36.
- [5] Swaminathan S, Fonseca VA, Alam MG, Shah SV. The role of iron in diabetes and its complications. *Diabetes Care* 2007;30:1926–33.
- [6] Narayanaswamy N, Govindaraju T. Aldazine-based colorimetric sensors for Cu²⁺ and Fe³⁺. *Sens Actuat B Chem* 2012;161:304–10.

- [7] Shamspur T, Sheikhshoae I, Mashhadizadeh MH. Flame atomic absorption spectroscopy (FAAS) determination of iron (III) after pre-concentration onto modified analcime zeolite with 5-((4-nitrophenylazo)-N-(2,4-dimethoxyphenyl)) salicylaldehyde by column method. *J Anal At Spectrom* 2005;20:476–8.
- [8] Timerbaev AR, Dabek-Zlotorzynska E, Hoop M. Inorganic environmental analysis by capillary electrophoresis. *Analyst* 1999;124:811–26.
- [9] Vanloot P, Coulomb B, Brach-Papa C, Sergent M, Boudenne JL. Multivariate optimization of solid-phase extraction applied to iron determination in finished waters. *Chemosphere* 2007;69:1351–60.
- [10] Yi C, Tian WW, Song B, Zheng YP, Qi ZJ, Qi Q, et al. A new turn-off fluorescent chemosensor for iron(III) based on new diphenylfluorenes with phosphonic acid. *J Lumin* 2013;141:15–22.
- [11] Cherreddy NR, Suman K, Korrapati PS, Thennarasu S, Mandal AB. Design and synthesis of rhodamine based chemosensors for the detection of Fe^{3+} ions. *Dyes Pigm* 2012;95:606–13.
- [12] Meng XL, Zhang X, Yao JS, Zhang JJ, Ding BY. Fluorescence and fluorescence imaging of two Schiff derivatives sensitive to Fe^{3+} induced by single- and two-photon excitation. *Sens Actuat B* 2013;176:488–96.
- [13] Bhalla V, Sharma N, Kumar N, Kumar M. Rhodamine based fluorescence turn-on chemosensor for nanomolar detection of Fe^{3+} ions. *Sens Actuat B* 2013;178:228–32.
- [14] She MY, Yang Z, Yin B, Zhang J, Gu J, Yin WT, et al. A novel rhodamine-based fluorescent and colorimetric “off-on” chemosensor and investigation of the recognizing behavior towards Fe^{3+} . *Dyes Pigm* 2012;92:1337–43.
- [15] Kumar M, Kumar R, Bhalla V. Optical chemosensor for Ag^+ , Fe^{3+} , and cysteine: information processing at molecular level. *Org Lett* 2011;13:366–9.
- [16] Yao JN, Dou W, Qin WW, Liu WS. A new coumarin-based chemosensor for Fe^{3+} in water. *Inorg Chem Comm* 2009;12:116–8.
- [17] Peng RG, Wang F, Sha YW. Synthesis of 5-Dialkyl(aryl)aminomethyl-8-hydroxyquinoline dansylates as selective fluorescent sensors for Fe^{3+} . *Molecules* 2007;12:1191–201.
- [18] Danjou PE, Lyskawa J, Delattre F, Becuwe M, Woisel P, Ruellan S, et al. New fluorescent and electropolymerizable N-azacrown carbazole as a selective probe for iron (III) in aqueous media. *Sens Actuat B* 2012;171–172:1022–8.
- [19] Bhardwaj VK, Pannu APS, Singh N, Hundal MS, Hundal G. Synthesis of new tripodalreceptorsda ‘PET’ based ‘off-on’ recognition of Ag^+ . *Tetrahedron* 2008;64:5384–91.
- [20] Pasco SI, Balazs G, Green JC, Green MLH, Vei IC, Warren JE, et al. Synthesis and structural investigations of Ni(II)- and Pd(II)-coordinated-diimines with chlorinated backbones. *Inorg Chim Acta* 2010;363:1157–72.
- [21] Ren J, Zhao XL, Wang QC, Ku CF, Qu DH, Chang CP, et al. Synthesis and fluorescence properties of novel co-facial folded naphthalimide dimers. *Dyes Pigm* 2005;64:179–86.
- [22] Li Y, Cao LF, Tian H. Fluoride ion-triggered dual fluorescence switch based on naphthalimides winged zinc porphyrin. *J Org Chem* 2006;71:8279–82.
- [23] Leng B, Tian H. A unimolecular half-subtractor based on effective photoinduced electron transfer and intramolecular charge transfer processes of 1,8-naphthalimide derivative. *Aust J Chem* 2010;63:169–72.
- [24] Reddy TS, Ram Reddy A. Synthesis and fluorescence study of 3-amino-alkylamidonaphthalimides. *J Photochem Photobiol A Chem* 2012;227:51–8.
- [25] Wu JS, Liu WM, Zhuang XQ, Wang F. Fluorescence turn-on of coumarin derivatives by metal cations: a new signaling mechanism based on C=N isomerization. *Org Lett* 2007;9:33–6.
- [26] Jayabharathi J, Thanikachalam V, Jayamoorthy K. Effective fluorescent chemosensors for the detection of Zn^{2+} metal ion. *Spectrochim Acta A* 2012;95:143–7.
- [27] Liu SR, Wu SP. New water-soluble highly selective fluorescent chemosensor for Fe (III) ions and its application to living cell imaging. *Sens Actuat B* 2012;171–172:1110–6.
- [28] Zhu M, Yuan MJ, Liu XF, Xu JL, Lv J, Huang CS, et al. A visible near-infrared chemosensor for mercury ion. *Org Lett* 2008;10:1481–4.